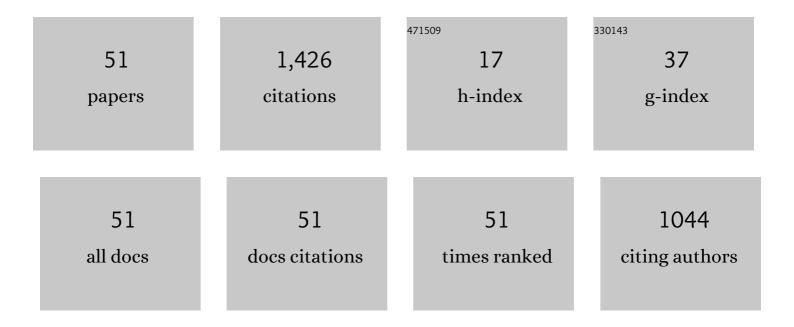
Zhan-Yong Zhao

List of Publications by Year in descending order

Source: https://exaly.com/author-pdf/1340224/publications.pdf Version: 2024-02-01



#	Article	IF	CITATIONS
1	High-Temperature Oxidation Behavior of NiCoCrAlY Coatings Deposited by Laser Cladding on 304 Stainless Steel. Metals and Materials International, 2022, 28, 412-420.	3.4	6
2	Effect of Heat Treatment on the Microstructure and Properties of Inconel 718 Alloy Fabricated by Selective Laser Melting. Journal of Materials Engineering and Performance, 2022, 31, 353-364.	2.5	5
3	Fabrication of magnesium-coated graphene and its effect on the microstructure of reinforced AZ91 magnesium-matrix composites. Advanced Composites and Hybrid Materials, 2022, 5, 504-512.	21.1	23
4	EBSD investigation on the microstructure of Ti48Al2Cr2Nb alloy hot isostatic pressing formed by Selective laser melting (SLM). Materials Letters, 2022, 309, 131334.	2.6	7
5	AZ91 alloy nanocomposites reinforced with Mg-coated graphene: Phases distribution, interfacial microstructure, and property analysis. Journal of Alloys and Compounds, 2022, 902, 163484.	5.5	41
6	Effect of Solution Temperature on the Microstructure and Properties of 17-4PH High-Strength Steel Samples Formed by Selective Laser Melting. Metals, 2022, 12, 425.	2.3	6
7	First Principle Study of MgSnLa Compounds in Mg-3Sn-1Mn-1La Alloy Processed by Rheo-Rolling. Materials, 2022, 15, 1361.	2.9	1
8	Microstructure and Properties of Porous 17-4PH Stainless Steel Prepared by Selective Laser Melting. Transactions of the Indian Institute of Metals, 2022, 75, 1641-1648.	1.5	3
9	Solidified behavior and microstructure of highÂstrengthÂAl–Mg alloy under electromagnetic field simulated by direct current. Journal of Materials Research, 2022, 37, 1115-1124.	2.6	0
10	Three-dimensional printing of the copper sulfate hybrid composites for supercapacitor electrodes with ultra-high areal and volumetric capacitances. Advanced Composites and Hybrid Materials, 2022, 5, 1537-1547.	21.1	78
11	Microstructure evolution of Zn–0.2Mg–0.8Mn(wt-%) alloys with different initial textures during room-temperature compression. Materials Science and Technology, 2022, 38, 1368-1375.	1.6	1
12	The interfacial structure of α-Ti/TiC in graphene-reinforced Ti6Al4V matrix composite coating prepared by laser cladding: first-principles and experimental. Applied Physics A: Materials Science and Processing, 2021, 127, 1.	2.3	3
13	Effects of alloying elements X (Cr, Mn, Mo, Ni, Si) on the interface stability of TiC (001)/γ-Fe (001) in TiC/316L stainless steel composite formed by selective laser melting: first principles and experiments. Advanced Composites and Hybrid Materials, 2021, 4, 195-204.	21.1	30
14	Microstructure and Properties of In situ Synthesized TiC/Graphene/Ti6Al4V Composite Coating by Laser Cladding. Transactions of the Indian Institute of Metals, 2021, 74, 891-899.	1.5	6
15	First Principle Study of TiB2 (0001)/Î ³ -Fe (111) Interfacial Strength and Heterogeneous Nucleation. Materials, 2021, 14, 1573.	2.9	8
16	Microstructure and properties of periodic porous Inconel 718 alloy prepared by selective laser melting. Advanced Composites and Hybrid Materials, 2021, 4, 332-338.	21.1	18
17	Tribological Behavior of In Situ TiC/Graphene/Graphite/Ti6Al4V Matrix Composite Through Laser Cladding. Acta Metallurgica Sinica (English Letters), 2021, 34, 1317-1330.	2.9	38
18	First-Principles Study on Graphene/Mg2Si Interface of Selective Laser Melting Graphene/Aluminum Matrix Composites. Metals, 2021, 11, 941.	2.3	3

ZHAN-YONG ZHAO

#	Article	IF	CITATIONS
19	Interfacial structures and strengthening mechanisms of in situ synthesized TiC reinforced Ti6Al4V composites by selective laser melting. Ceramics International, 2021, 47, 34127-34136.	4.8	21
20	Compression properties of porous Inconel 718 alloy formed by selective laser melting. Advanced Composites and Hybrid Materials, 2021, 4, 1309-1321.	21.1	9
21	Deformation strengthening mechanism of in situ TiC/TC4 alloy nanocomposites produced by selective laser melting. Composites Part B: Engineering, 2021, 225, 109305.	12.0	29
22	Wear resistance of graphene nano-platelets (GNPs) reinforced AlSi10Mg matrix composite prepared by SLM. Applied Surface Science, 2020, 503, 144156.	6.1	87
23	Failure Analysis of the Tree Column Structures Type AlSi10Mg Alloy Branches Manufactured by Selective Laser Melting. Materials, 2020, 13, 3969.	2.9	3
24	Microstructure characterisation of in-situ synthesised TiC/Ti6Al4 V composite coating by laser cladding. Philosophical Magazine Letters, 2020, 100, 588-595.	1.2	1
25	Interfacial Stability of TiC/γ-Fe in TiC/316L Stainless Steel Composites Prepared by Selective Laser Melting: First Principles and Experiment. Metals, 2020, 10, 1225.	2.3	7
26	Formability and hardness studies of selective laser melting of GH4169 Ni-based alloy powders. Emerging Materials Research, 2020, 9, 758-769.	0.7	2
27	The Compressive Behavior of Porous TC4 Alloy Scaffolds Manufactured by Selective Laser Melting. Transactions of the Indian Institute of Metals, 2020, 73, 2861-2867.	1.5	9
28	An overview of graphene and its derivatives reinforced metal matrix composites: Preparation, properties and applications. Carbon, 2020, 170, 302-326.	10.3	169
29	The Evolution of Microstructure, Mechanical Properties and Fracture Behavior with Increasing Lanthanum Content in AZ91 Alloy. Metals, 2020, 10, 1256.	2.3	7
30	Influence of rhenium and tungsten on the microstructure and performance of GH4169 alloy through heat treatment. Emerging Materials Research, 2020, 9, 705-715.	0.7	1
31	The Interfacial Characteristics of Graphene/Al4C3 in Graphene/AlSi10Mg Composites Prepared by Selective Laser Melting: First Principles and Experimental Results. Materials, 2020, 13, 702.	2.9	14
32	In-situ synthesis of TiC/graphene/Ti6Al4V composite coating by laser cladding. Materials Letters, 2020, 270, 127711.	2.6	33
33	Microstructure and tribological behavior of graphene/Al composites produced by selective laser melting. Materials Research Express, 2019, 6, 1065c1.	1.6	17
34	Tribological Behavior of TiC Particles Reinforced 316Lss Composite Fabricated Using Selective Laser Melting. Materials, 2019, 12, 950.	2.9	17
35	AlSi10Mg alloy nanocomposites reinforced with aluminum-coated graphene: Selective laser melting, interfacial microstructure and property analysis. Journal of Alloys and Compounds, 2019, 792, 203-214.	5.5	147
36	The Reaction Thermodynamics during Plating Al on Graphene Process. Materials, 2019, 12, 330.	2.9	43

ZHAN-YONG ZHAO

#	Article	IF	CITATIONS
37	Microstructure and Mechanical Properties of TiC-Reinforced 316L Stainless Steel Composites Fabricated Using Selective Laser Melting. Metals, 2019, 9, 267.	2.3	71
38	Microstructural evolution and mechanical properties of IN718 alloy fabricated by selective laser melting following different heat treatments. Journal of Alloys and Compounds, 2019, 772, 861-870.	5.5	108
39	Microstructure and properties of Ti/TiBCN coating on 7075 aluminum alloy by laser cladding. Surface and Coatings Technology, 2018, 334, 142-149.	4.8	63
40	Friction and wear behaviour of Inconel 718 alloy fabricated by selective laser melting after heat treatments. Philosophical Magazine Letters, 2018, 98, 547-555.	1.2	10
41	Temperature distribution and its influence on microstructure of Mg–3Sn–1Mn alloy during rheo-rolling process. Philosophical Magazine, 2018, 98, 2367-2379.	1.6	2
42	Analysis of Geometrical Characteristics and Properties of Laser Cladding 85 wt.% Ti + 15 wt.% TiBCN Powder on 7075 Aluminum Alloy Substrate. Materials, 2018, 11, 1551.	2.9	14
43	Simulation of Stress Field during the Selective Laser Melting Process of the Nickel-Based Superalloy, GH4169. Materials, 2018, 11, 1525.	2.9	19
44	Microstructural evolution and mechanical strengthening mechanism of Mg-3Sn-1Mn-1La alloy after heat treatments. Materials Science & Engineering A: Structural Materials: Properties, Microstructure and Processing, 2018, 734, 200-209.	5.6	91
45	The Heat Treatment Influence on the Microstructure and Hardness of TC4 Titanium Alloy Manufactured via Selective Laser Melting. Materials, 2018, 11, 1318.	2.9	64
46	Effects of Process Parameters of Semisolid Stirring on Microstructure of Mg–3Sn–1Mn–3SiC (wt%) Strip Processed by Rheo-rolling. Acta Metallurgica Sinica (English Letters), 2017, 30, 66-72.	2.9	76
47	Formation of yittrium oxide in cemented carbides. Philosophical Magazine Letters, 2017, 97, 469-475.	1.2	1
48	Microstructure and deformation behavior of Ti-10V-2Fe-3Al alloy during hot forming process. Journal Wuhan University of Technology, Materials Science Edition, 2015, 30, 1332-1337.	1.0	1
49	Mathematical model and theoretical research of flow shear constitutive relation during rheo-rolling of semisolid alloy. Journal Wuhan University of Technology, Materials Science Edition, 2015, 30, 1049-1055.	1.0	0
50	Boundary layer distributions and cooling rate of cooling sloping plate process. Journal Wuhan University of Technology, Materials Science Edition, 2013, 28, 701-705.	1.0	5
51	Microstructure evolution and solidification behaviors of A2017 alloy during cooling/stirring and rolling process. Transactions of Nonferrous Metals Society of China, 2012, 22, 2871-2876.	4.2	8